Available online at www.sciencedirect.com
ScienceDirect
Journal of Molecular Catalysis A: Chemical 277 (2007) 1–14
JOURNAL OF MOLECULAR CATALYSIS A: CHEMICAL
www.elsevier.com/locate/molcata

Editor Choice paper

Effects of acid properties of Y zeolites on the liquid-phase alkylation of benzene with 1-octene: A reaction path analysis

Ionel Craciun, Marie-Françoise Reyniers *, Guy B. Marin

Laboratorium voor Petrochemische Techniek, Ghent University, Krijgslaan 281(S5), B-9000 Gent, Belgium

Received 25 May 2007; received in revised form 26 June 2007; accepted 27 June 2007
Available online 10 July 2007

Abstract

The liquid-phase alkylation of benzene with 1-octene was investigated over three USY zeolites with bulk Si/Al ratios of 6, 13 and 30, at temperatures ranging from 343 K to 373 K, benzene/1-octene feed molar ratios ranging from 1 to 10 and 1-octene conversions between 10% and 99%. 2-, 3- and 4-octene isomers are formed consecutively from double bond isomerization of 1-octene; 2-, 3- and 4-phenyloctanes are obtained as alkylated products. Catalyst deactivation is less important at 1-octene conversions higher than 90%. Reaction path analysis reveals that on the fresh catalyst double bond isomerization and benzene alkylation occur on comparable time scales necessitating the simultaneous consideration of all elementary steps involved in the formation of linear alkylbenzenes. Only 2-octene and 2-phenyloctane are identified as primary products. The higher initial selectivity to 2-octene as compared to 2-phenyloctane is related to differences in entropy of activation associated with deprotonation and alkylation steps. The catalytic activity increases with increasing Si/Al ratio while the selectivities are not affected. The higher rates observed for the catalyst with the higher average acid strength can be traced back to a decrease in the activation energy for the protonation step leading to an increased concentration of carbenium ions on the catalyst surface that compensates for the higher activation energies for the deprotonation and alkylation steps. The constant selectivities are explained by a similar dependency of the different elementary steps on the acid site strength.

Keywords: Linear alkylbenzenes; Alkylation; Double bond isomerization; Benzene; Octene; USY; Y zeolite; Acid strength; Acid catalysis

1. Introduction

Alkylbenzenes are large-scale chemicals obtained by acid catalyzed alkylation of the aromatic ring. Traditionally, these compounds were obtained by Friedel-Crafts reactions using homogeneous acid catalysts. Even today Friedel-Crafts catalysts still play an important role in the manufacturing of alkyl-substituted aromatics. Homogeneous catalysts such as $AlCl_3$ and HF are used extensively in the detergent industry for the production of linear alkylbenzenes (LAB), although they suffer from a series of technical and environmental drawbacks. The use of a solid acid as heterogeneous catalyst offers several advantages and in the last four decades, significant progress has been made towards the development of improved industrial alkylation processes. A large number of materials have been tested as catalysts for the alkylation of aromatics. They include homogeneous catalysts immobilized on solid supports [1,2], silica–aluminas [3–6], clays [3], heteropolyacids [7,8] and metal oxides [9]. A special class of materials that were found to perform particularly well in alkylation is constituted by zeolites and modified zeolites such us beta [3,10–15], Y [3,16–20], MCM-22 [14,21] and mordenite [3,22,23].

A major breakthrough in the industrial production of ethylbenzene with a solid acid catalyst was achieved by Mobil-Badger in 1976 using a ZSM-5 zeolite in a gas phase fixed-bed reactor [24]. Other companies followed and developed or improved their own technologies for the production of ethylbenzene using solid catalysts [25,26]. Besides ZSM-5, Y zeolite and MCM-22 are reported to be the most successful solid acid catalysts for the gas phase alkylation of benzene with ethylene [26]. Nowadays, less than 25% of the global ethylbenzene production relies on the traditional $AlCl_3$–HF technology [26]. For the production of linear alkylbenzenes, however, the traditional HF-catalyzed process, developed by UOP [27], still dominates the market. Recently, UOP started to commercialize the newly developed Detal^{TM} process for the liquid-phase alkylation of benzene with olefins in mild conditions [28], using a fluoride-based catalyst [5], named DA-114, in a cyclic fixed bed axial flow reactor.

* Corresponding author. Tel.: +32 9 2644516; fax: +32 9 2644999.
E-mail address: MarieFrancoise.Reyniers@UGent.be (M.-F. Reyniers).

1381-1169/$ – see front matter © 2007 Elsevier B.V. All rights reserved.
doi:10.1016/j.molcata.2007.06.027

Nomenclature

List of symbols

A_{alk}	preexponential factor for surface alkylation step ($m^3\ mol^{-1}\ s^{-1}$)
$A_{de\text{-}pr}$	preexponential factor for deprotonation step (s^{-1})
BAL_C	carbon atom balance (%)
C	molar concentration ($mol\ m^{-3}$)
C_t	total concentration of acid active sites ($mol\ kg_{cat}^{-1}$)
$E_{a,alk}$	activation energy for surface alkylation step ($kJ\ mol^{-1}$)
$E_{a,de\text{-}pr}$	activation energy for deprotonation step ($kJ\ mol^{-1}$)
$E_{a,pr}$	activation energy for protonation step ($kJ\ mol^{-1}$)
$\Delta(E_{a,alk})$	difference in activation energies for alkylation step on two different catalysts ($kJ\ mol^{-1}$)
$\Delta(E_{a,pr})$	difference in activation energies for protonation step on two different catalysts ($kJ\ mol^{-1}$)
ΔH_{pr}	1-octene protonation enthalpy on catalyst ($kJ\ mol^{-1}$)
$\Delta(\Delta H_{pr})$	difference in octene protonation enthalpies on two different catalysts ($kJ\ mol^{-1}$)
F	molar flow rate ($mol\ s^{-1}$)
k_{alk}	rate coefficient for surface alkylation step ($m^3\ mol^{-1}\ s^{-1}$)
$k_{de\text{-}pr}$	rate coefficient for deprotonation step (s^{-1})
$K_{eq,iso}$	equilibrium coefficient for the isomerization of 1-octene to 2-octene (−)
k_{pr}	rate coefficient for protonation step ($m^3\ mol^{-1}\ s^{-1}$)
$K_{pr,1\text{-}oct}$	equilibrium coefficient for 1-octene protonation to 2-octyl carbenium ion ($m^3\ mol^{-1}$)
$K_{pr,2\text{-}oct}$	equilibrium coefficient for 2-octene protonation to 2-octyl carbenium ion ($m^3\ mol^{-1}$)
$\dot{m}$	mass flow rate ($kg\ s^{-1}$)
M_W	molar weight ($kg\ mol^{-1}$)
n_c	number of carbon atoms in molecule
N_{H^+}	number of acid sites (mol)
R	net consumption/production rate ($mol\ kg_{cat}\ s^{-1}$)
S	selectivity (%)
T	temperature (K)
w	weight fraction (−)
W_{cat}	catalyst mass (kg)
X	conversion (%)
Y	molar yield (%)

Greek letter

α	parameter in Polanyi relation (Eq. (25))

Superscript

0	initial (feed) condition

Subscripts

A, B	over catalyst A, respectively, B
b	benzene
i, j	general component
i,oct	pertaining to general component, i, calculated with respect to all octenes
i-oct	i-octene ("i" positional isomer of octene)
i-pho	i-phenyloctane ("i" positional isomer of phenyloctane)
max	maximum value
oct	octenes (sum of all positional isomers of octene)
tot	total

Three units based on the Detal™ technology and the DA-114 catalysts were already in commercial operation in 2003 [29].

In view of the increasing concern for environmental issues, polluting technologies are bound to yield to newer, economically viable, environmental friendlier technologies. Unfortunately, among the large variety of materials with acidic properties tested in the alkylation of aromatics [1–22], only few have found industrial valorization. For industrial application high selectivity to the linear 2-phenyl isomer is the major target as this isomer yields detergents with better emulsifying properties and better biodegradability [30,31]. Generally, high conversions can be easily obtained using acid catalysts but the product distribution can vary strongly. Depending on the properties of the catalyst, all isomers of the mono-alkylated products can be formed during the alkylation even when starting from the 1-olefins. This is caused by the concurrent branching and double bond isomerization of the olefins. Other possible by-products that have been reported result from poly-alkylation and from the isomerization and oligomerization of olefins. Knowledge of the influence of the different experimental parameters on the product range obtained in the alkylation offers an important tool in the development of more efficient industrial processes [32,33].

In this paper, the liquid-phase alkylation of benzene with C_8 linear olefins over a series of Y zeolites was chosen as model reaction to evaluate the influence of temperature, feed molar ratio, space time and catalyst Si/Al ratio, on the conversion and the product distribution. Y is a large pore zeolite with a tri-dimensional network of channels with diameter of 7.4 Å at the intersection of which cavities with diameters of 11.8 Å are formed. This zeolite combines two important features that make it suitable as catalyst for the alkylation of benzene with long-chain olefins: strong acidic character and the ability to accommodate large molecules, such as alkylbenzenes, inside its pores. Moreover, its thermal stability and catalytic activity can be improved by dealumination [17,18]. Dealmeida et al. [16] reported the effect of the aluminum content on the alkylation of benzene with 1-dodecene over HY-zeolites performed in a batch–slurry reactor and concluded that the selectivity to 2-phenyldodecane increased with increasing acid strength. However, HY-zeolites are prone to deactivation and operation in batch mode does not allow excluding the influence of coke deposition on the product distribution. In this study, the alkylation of benzene with 1-octene was performed in a Robinson–Mahoney reactor operating in a continuous flow mode allowing extrapolation to zero time on stream and thus enabling the determination

of the influence of process conditions and of the acid properties on the activity and selectivity in the absence of deactivation. Based on the experimental observations, a detailed reaction mechanism has been developed and the influence of the acid characteristics of the fresh catalyst on the product distribution is evaluated.

2. Experimental

2.1. Materials

Three commercially available ultrastable Y zeolites, CBV712 ($Si/Al_{bulk} = 6$), CBV720 ($Si/Al_{bulk} = 13$), and CBV760 ($Si/Al_{bulk} = 30$) were purchased from Zeolyst International. These zeolites were obtained by dealumination, to different degrees, of a parent Y zeolite with Si/Al = 2.6 denominated commercially CBV300. The CBV720 and CBV760 zeolites were supplied in H-form while CBV712 was supplied in ammonia form. A detailed characterization of the catalysts is given elsewhere [34–37] and the relevant properties are summarized in Table 1.

Benzene (bp, 80.1 °C; purity, >99.5%) and 1-octene (bp, 121.3 °C; purity > 99.5%) have been purchased from Acros Organics, Belgium, and used without further purification. A mixture of octene isomers containing 21.8% 1-octene, 50.0% 2-octene, 25.1% 3-octene, 1.1% 4-octene and 2.0% other hydrocarbons impurities, used in a series of experiments with mixed olefin feed, was synthesized by contacting 1-octene with CBV760 for 3 h in a glass reactor, under reflux conditions.

3. Experimental procedure

The experimental tests were performed in a set-up operating in continuous flow mode, including a Robinson–Mahoney reactor (Autoclave Engineers, Europe). The particularity of this type of reactor is the use of a specially designed "basket" in which the catalyst is contained, while a specially designed stirrer forces the content of the reactor through the basket walls ensuring a high degree of internal recirculation [38]. The set-up and the operational procedures are designed to avoid contact with the carcinogenic benzene component. To prevent exposure in case of an accidental release of benzene, the set-up is equipped with a powerful ventilation system and liquid collection vessels.

Table 1
Characteristics of the Y zeolite catalysts used in liquid-phase alkylation of benzene with 1-octene

	CBV712	CBV720	CBV760
Bulk Si/Al ratio[a]	5.8	13	30
Micropore volume (cm^3/g)[b]	0.251	0.273	0.250
Mesopore volume (cm^3/g)[b]	–	0.15	0.16
External surface (m^2/g)[b]	109	103	143
Acid site concentration (mmol/g)[c]	0.69	0.62	0.24
Al (IV) content (mmol/g)[d]	0.75	0.613	0.217
a_o (nm)[e]	24.36	24.34	24.25
Total Al/uc[f]	28.2	13.7	6.2
Framework Al/uc[g]	8.6	7.1	2.5
Framework Si/Al ratio	21.2	26.2	75.8

[a] Determined by ICPS (inductively coupled plasma spectroscopy) [35,38].
[b] Determined with nitrogen porosimetry at 77 K (procedure proposed by Remy [38]).
[c] Determined with ammonia TPD [36,37].
[d] Determined with Al MAS NMR [35,38].
[e] Calculated from the X-ray diffraction spectrum using the ASTM procedure D 4932-85 [38].
[f] Calculated from the total Al content (determined by ICPS) assuming a unit cell composition of $H_x(AlO_2)_x(SiO_2)_{192-x}$.
[g] Calculated from the number of Al(IV) species per gram catalyst (determined by Al MAS NMR) assuming a unit cell composition of $H_x(AlO_2)_x(SiO_2)_{192-x}$.

For a typical experiment, the catalyst, supplied as powder, is first pressed into wafers using a hydraulic press. The wafers are then crushed and the resulting pellets are sieved; only the fraction of particles with diameters between 0.5 mm and 0.6 mm are used in the experiments. Prior to its use in catalytic experiments, the catalyst is activated at 723 K in a down-flow fixed-bed reactor, under 20 ml/min airflow. The catalyst is kept at this temperature for 4 h to eliminate water and other contaminants that could have been adsorbed from the laboratory atmosphere. Prior to this treatment, CBV712, supplied in ammonia form, spent an additional night at 773 K, under air, in order to obtain the H-form. After activation, the desired amount of catalyst is weighted (W = 1–10 g), diluted with α-alumina (dilution = 1 g catalyst/10 g α-alumina) and loaded into the catalyst basket. After the catalyst basket is introduced into the reactor, the reactor is closed and the catalyst is submitted to an overnight in situ activation under 20 ml/min airflow, at 623 K, to remove traces of contaminants adsorbed during the loading of the reactor. Once the catalyst is activated, the temperature of the reactor is set to the desired value. After the equilibration of the temperature in the set-up, the air flow is stopped and the reactor pressure is brought to 2 MPa by means of a N_2 flow. Throughout the experiment the reactor is kept at 2 MPa. At this pressure all reactants and reaction products are in liquid-phase at all experimental conditions investigated.

The reactant mixture of the desired composition is fed to the reactor by means of a HPLC pump. The HPLC pump delivers a constant feed flow rate to the reactor; the mass flow rate is verified on a regular basis by means of a Sartorius balance. A stirrer revolution speed of 2000 rpm was used to ensure perfect mixing inside the reactor. The reactor effluent is collected first in a measuring burette and subsequently in a closed recipient whose mass is monitored by means of a Sartorius balance. For each experimental test, 0.3 ml samples of the reactor effluent are withdrawn at every 15–30 min time on stream and analyzed off-line by means of a HP5890 Series II Gas Chromatograph equipped with a CP-SIL-5 capillary column (50 m, 0.32 mm, 5.0 μm) and a flame ionization detector.

The chromatographic analysis of the gaseous fraction of the reactor content, by injecting on-line samples of a gaseous effluent stream mixed with a known CH_4 flow rate, revealed that no light components are formed during reaction.

The flash gas, desorbed when the liquid effluent exits the high-pressure section of the installation, consists of only N_2 as revealed by the gas chromatograph analysis of off-line injected samples.

Based on the above-mentioned observations, the outlet molar flow rates of the individual components are calculated starting

from the GC analysis of the reactor liquid effluent and the mass flow rate of the reactor effluent

$$F_i = \frac{w_i \dot{m}_{\text{tot}}}{M_{\text{W}_i}} \tag{1}$$

with F_i is the outlet molar flow rate of a component "i", w_i the mass fraction of component "i" in the reactor effluent, M_{W_i} the molar weight of component "i" and $\dot{m}_{\text{tot}}$ is the total mass flow rate of the effluent.

The activity of the catalyst is expressed by the conversion of 1-octene, $X_{\text{1-oct}}$, defined as

$$X_{\text{1-oct}} = \frac{F^0_{\text{1-oct}} - F_{\text{1-oct}}}{F^0_{\text{1-oct}}} \tag{2}$$

with $F^0_{\text{1-oct}}$ and $F_{\text{1-oct}}$ are the feed, respectively outlet, molar flow rates of 1-octene.

The overall octenes conversion, X_{oct}, is defined as

$$X_{\text{oct}} = \frac{\sum_{j=1}^{4}(F^0_{j\text{-oct}} - F_{j\text{-oct}})}{\sum_{j=1}^{4} F^0_{j\text{-oct}}} \tag{3}$$

where $F^0_{j\text{-oct}}$ and $F_{j\text{-oct}}$ are the feed, respectively outlet, molar flow rates of "j"-octene isomer.

The molar yield of a reaction product i, Y_i, is calculated with respect to 1-octene, as moles of product "i" produced per mole 1-octene fed. In terms of molar flow rates this is expressed as

$$Y_i = \frac{F_i - F^0_i}{F^0_{\text{1-oct}}} \tag{4}$$

with F^0_i and F_i are the feed, respectively outlet, molar flow rates of component "i", and $F^0_{\text{1-oct}}$ is the inlet molar flow rate of 1-octene.

Selectivity towards a product "i" with respect to 1-octene, S_i, is defined as moles of product "i" formed per mole of 1-octene converted. In terms of molar flow rates, the selectivity with respect to 1-octene is expressed by

$$S_i = \frac{F_i - F^0_i}{F^0_{\text{1-oct}} - F_{\text{1-oct}}} \tag{5}$$

For the selectivity to a product "i", calculated with respect to the total amount of olefins consumed ($S_{i,\text{oct}}$), the following equation applies

$$S_{i,\text{oct}} = \frac{F_i - F^0_i}{\sum_{j=1}^{4}(F^0_{j\text{-oct}} - F_{j\text{-oct}})} \tag{6}$$

The net 1-octene consumption rate, $R_{\text{1-oct}}$ and the net production rate of a product "i", R_i, in mol s^{-1} $\text{kg}^{-1}_{\text{cat}}$, can be obtained by dividing the 1-octene conversion (Eq. (2)) and the molar yield of product "i" (Eq. (4)) by the corresponding space time, $W_{\text{cat}}/F^0_{\text{1-oct}}$

$$R_{\text{1-oct}} = \frac{X_{\text{1-oct}}}{W_{\text{cat}}/F^0_{\text{1-oct}}} \tag{7}$$

$$R_i = \frac{Y_i}{W_{\text{cat}}/F^{\text{o}}_{\text{1-oct}}} \tag{8}$$

where the space time is defined as the mass of catalyst, W_{cat}, divided by the inlet molar flow rate of the 1-octene reactant, $F^0_{\text{1-oct}}$. Introducing site time, i.e. $N_{\text{H}^+}/F^0_{\text{1-oct}}$, allows comparing the different catalysts.

The number of acid sites, N_{H^+}, used in the above expression, is obtained taking into account the acid site concentrations, C_{t}, given in Table 1 for the investigated catalysts

$$N_{\text{H}^+} = C_{\text{t}} W_{\text{cat}} \tag{9}$$

The carbon balance is calculated based on the inlet and outlet molar flow rates of the individual components

$$\text{BAL}_{\text{C}} = 100 \frac{\sum n_{\text{c}_i} F_i}{\sum n_{\text{c}_i} F^0_i} \tag{10}$$

where n_{c_i} represents the number of carbon atoms in component "i".

An overview of the experimental conditions is given in Table 2. Prior to the start of the experimental program, a blank test has been performed feeding a mixture of benzene and 1-octene in a molar ratio of 5:1 over a catalyst basket filled with α-alumina, at 473 K, for 10 h time on stream so that the activity of the diluting material could be investigated at severe experimental conditions. This test showed a 1-octene conversion of less than 0.5%, with the formation of traces of 2-octene. No traces of alkylated products were found.

For all experimental conditions the absence of mass and heat transport limitations was verified using correlations from literature [39].

The data reported in this paper refer to the fresh catalyst and were obtained by extrapolating the values of the conversions and molar yields, observed as a function of time on stream, to time on stream zero. A similar approach has been reported by Corma et al. [14] in the study of the kinetics of the alkylation of benzene with ethylene and propylene over an MCM-22 catalyst. The extrapolation is done by fitting an exponential function to the experimental points giving higher weight to the experimental points obtained at low time on stream.

The reported data pertain to experiments for which the carbon balance closes within $100 \pm 5\%$.

Table 2
Experimental conditions

Catalyst (Si/Al)	Temperature (K)	Benzene/1-octene feed molar ratio	Space time (kg s mol^{-1})	1-Octene conversion (%)
CBV712 (Si/Al = 5.8)	373	5	5–120	10–95
CBV720 (Si/Al = 13)	373–473	5	5–120	35–99
CBV760 (Si/Al = 30)	343–373	1–10	5–120	30–99

4. Results and discussion

4.1. Catalyst deactivation

Although the investigated Y zeolites show good performances as catalysts for the alkylation of benzene, their activity, expressed in terms of 1-octene conversions, decreases during time on stream. Generally, the deactivation of zeolite catalysts takes place by site coverage, when certain components, i.e. coke, strongly and irreversibly adsorb on the acid sites, and/or by pore blockage, when the bulky coke molecules hamper the access of reactants to the active sites [40,41].

In this study, it was observed that the deactivation of the catalyst is less important at high 1-octene conversions, i.e. >90% (Fig. 1). This observation indicates that mainly the olefins are responsible for the catalyst deactivation since at high 1-octene conversions, the selectivities to alkylated products are high resulting in low octenes concentration in the reaction mixture. As a consequence, secondary reactions involving octenes leading to deactivation are less important at high 1-octene conversions. Therefore, operating at high olefin conversions and high aromatic/olefin ratios increase the catalyst lifetime. An activity test performed at 473K and inlet benzene to 1-octene molar ratio of 5, at almost total octenes conversion ($X_{1\text{-oct}} = 99.5\%$, $X_{\text{oct}} = 98.5\%$), showed a decrease in the activity of CBV720 of less than 2% after 12 h time on stream.

4.2. Reaction network

As mentioned before, all data reported pertain to the fresh catalyst and were obtained by extrapolation to time on stream zero. For all catalysts and all experimental conditions investigated in this study, two main groups of components were obtained as reaction products: octene isomers and phenyloctanes. Branched octene isomers were not observed. The octene isomers, 2-octene, 3-octene and 4-octene, result from double bond migration. 2-Phenyloctane, 3-phenyloctane and 4-phenyloctane were obtained as mono-alkylated products. Traces of di-alkylated products (di-octylbenzenes), accounting for less than 1% of the 1-octene conversions, were obtained over CBV760 at 373K, $W_{\text{cat}}/F^0_{\text{1-oct}} = 10\,\text{kg s mol}^{-1}$ and low benzene

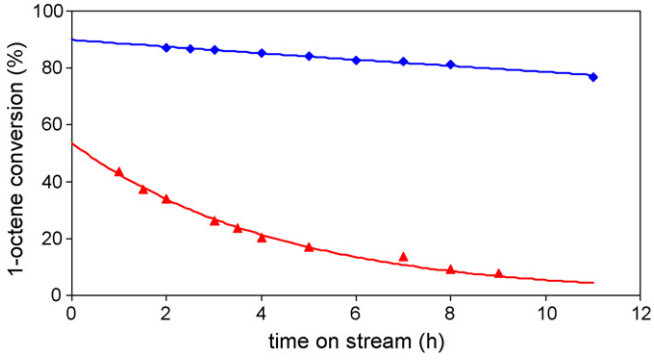

Fig. 1. 1-Octene conversion over CBV760 catalyst as a function of time on stream at 373 K and benzene/1-octene feed molar ratio = 5 ((♦) $w_{\text{cat}}/F^0_{\text{1-oct}} = 50\,\text{kg s mol}^{-1}$; (▲) $w_{\text{cat}}/F^0_{\text{1-oct}} = 5\,\text{kg s mol}^{-1}$).

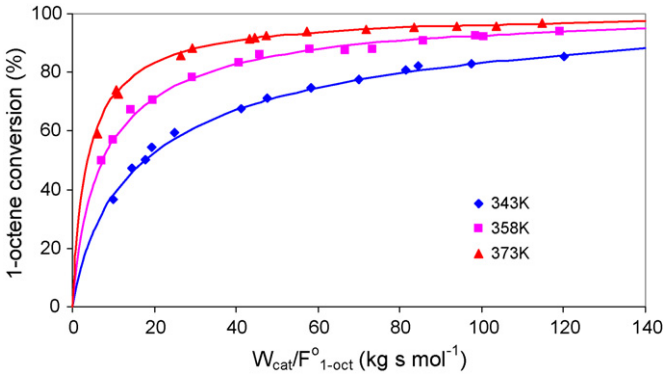

Fig. 2. Conversion of 1-octene over fresh CBV760 catalyst (t.o.s. = 0) at different temperatures and benzene/1-octene feed molar ratio = 5.

to 1-octene feed molar ratios (i.e. B/O = 1 and B/O = 3). In all conditions used in this study, octene dimers were not observed in the effluent.

Over CBV760, high levels of 1-octene conversions were obtained at all temperatures studied (Fig. 2). 2-Octene and 3-octene are the main reaction products formed at low space times (Fig. 3a). After an initial increase, the molar yields of the octene isomers decrease with increasing space time (Fig. 3a and b). Among the octene isomers, 2-octene is obtained in highest yields, followed by 3-octene and then 4-octene. However, low yields of 4-octene are obtained at all the experimental conditions investigated. The molar yields of the mono-alkylated products increase monotonically with increasing space time (Fig. 3c and d). Fig. 3 also shows that among the three mono-alkylated products, 2-phenyloctane – the most desired phenyloctane isomer – is always obtained with higher yields than 3-phenyloctane and 4-phenyloctane. A total molar yield of mono-alkylated products of 72% ($Y_{\text{2-pho,max}} = 29\%$, $Y_{\text{3-pho,max}} = 23\%$, $Y_{\text{4-pho,max}} = 20\%$) was obtained over CBV760 at the highest space time, $(W_{\text{cat}}/F^0_{\text{1-oct}})_{\text{max}} = 120\,\text{kg s mol}^{-1}$, and temperature, $T_{\text{max}} = 373\text{K}$, employed here.

The formation of these products from benzene and 1-octene can be explained based on the generally accepted mechanism involving the formation of an alkylcarbenium ion by the interaction of the olefin with the acid catalyst. The thus-formed carbocation then attacks the aromatic ring and forms an arenium ion – a so-called sigma-complex – in a step which is, in most cases, rate determining. In the final step, the sigma-complex eliminates, as a proton, the hydrogen bonded to the attacked aromatic carbon with the formation of the final alkylated product and the regeneration of the catalyst. Although, in the case of solid acid catalysts, the exact nature of the intermediate species is not yet precisely known, the alkylation of aromatics with olefins is commonly considered to involve a carbenium ion type mechanism equivalent to the one described above [16,17]—see Scheme 1. This mechanism explains the absence of the 1-phenyl-isomer among the reaction products, as its formation would involve the highly activated formation of a primary carbenium ion.

A schematic overview of the theoretical possible elementary reactions involving carbenium ions formed by protonation of the

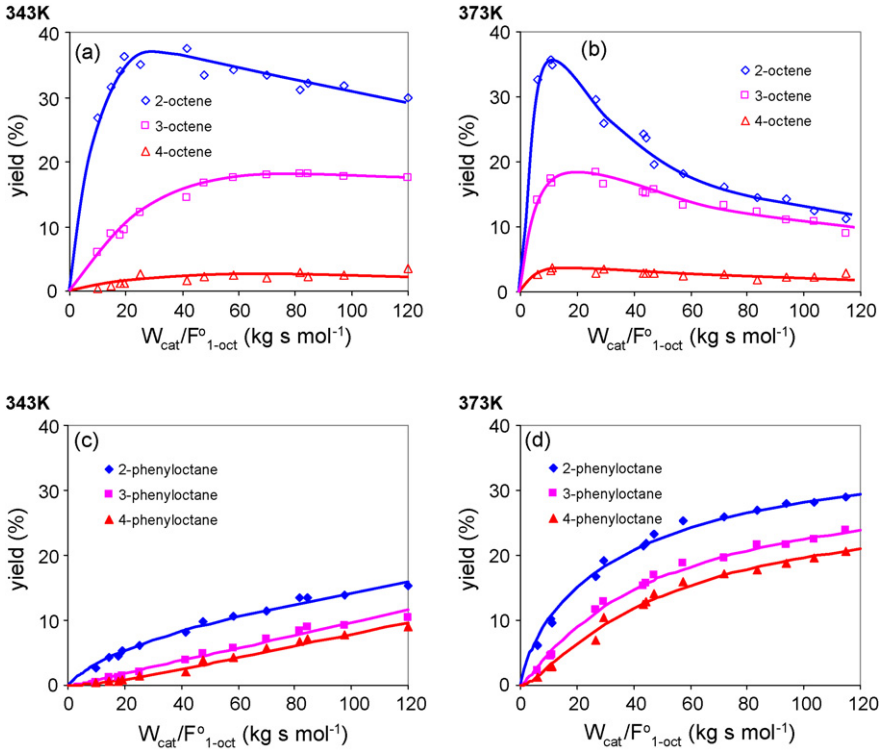

Fig. 3. Molar yields of octene isomers (a, b) and phenyloctanes (c, d) over fresh CBV760 catalyst (t.o.s. = 0) as a function of space time, at 343 K (left) and 373 K (right) and benzene/1-octene feed molar ratio = 5.

octenes on the acid sites of the zeolite is presented in Scheme 2. Acid catalyzed double bond isomerization results in the formation of 2-octene, 3-octene and 4-octene. The double bond isomerization can occur by a sequence of 1,2-hydride shifts of the 2-octyl carbenium ion leading to the 3-octyl and 4-octyl carbenium ions (Scheme 2b) followed by deprotonation and/or by a consecutive olefin protonation–deprotonation sequence involving the octyl carbenium ions as intermediates (Scheme 2a). The intermediate octyl carbenium ions react with benzene leading to 2-, 3- and 4-phenyloctane following the mechanism presented in Scheme 1.

Protonated cyclopropane (PCP) branching steps involving the secondary octyl carbenium ions can, in principle, result in the formation of branched olefins and/or branched alkylbenzenes (Scheme 2c). Cracking reactions involving the carbenium ions (Scheme 2d) can, in principle, also be expected [17]. However, none of the products expected from these reactions were observed at the experimental conditions investigated here. The absence of skeletal isomerization and cracking products can be explained based on the higher activation energies for the PCP branching and β-scission steps than for the double bond isomerization and alkylation steps over Y zeolites [32]. There-

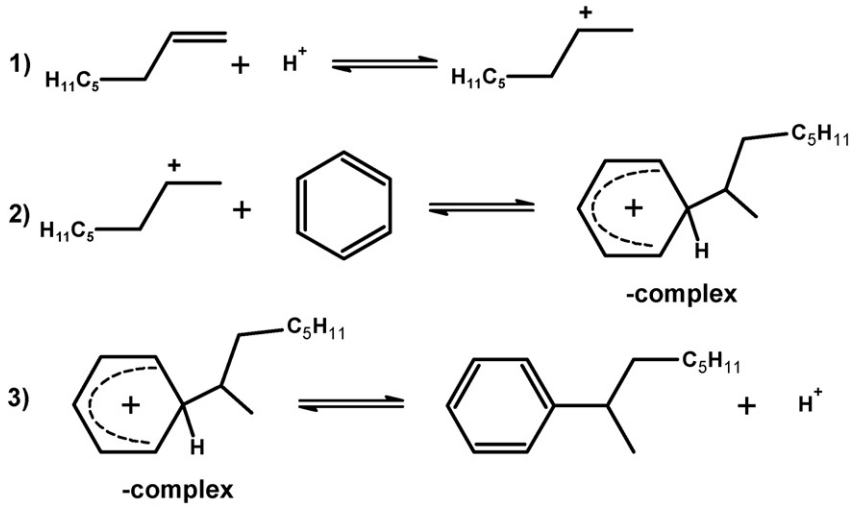

Scheme 1. Elementary steps involved in the alkylation of benzene with 1-octene over acid catalysts.

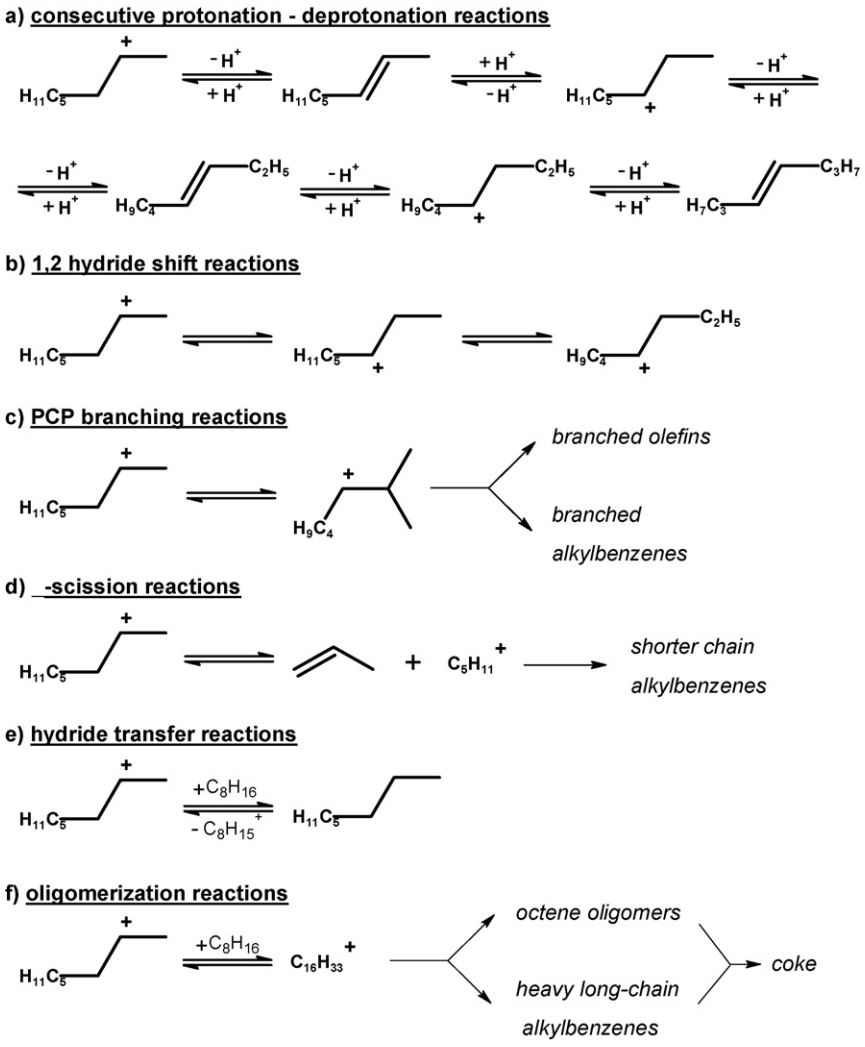

Scheme 2. Elementary reactions involving alkyl-carbenium ions.

fore, insignificant rates of C–C bond breaking reactions can be expected at the relatively low temperatures used in this study. As a consequence, the formation of branched alkylbenzenes is also highly unlikely.

At the experimental conditions investigated, i.e. at relatively low temperatures, hydride transfer reactions (Scheme 2e) do not occur noticeably—no alkanes were obtained among the reaction products.

Another reaction path involves the reaction of the carbenium ion intermediates with olefin molecules forming oligomeric species (Scheme 2f). Although octene oligomers have not been observed in the reactor effluent, the formation of oligomeric species that can be trapped inside the pores of the zeolites has been reported [42]. These oligomeric species are mainly responsible for the deactivation of the catalysts; either directly, by blocking the sites and the pores of the zeolite, or indirectly, by being the precursors for the formation of (other) coke molecules through further polymerization, alkylation and cyclization reactions.

Fig. 4a and b presents the selectivities to individual reaction products as a function of 1-octene conversion over CBV760 at 343K and feed molar ratio benzene/1-octene = 5. As the alkylation reaction is practically irreversible ($K \cong 10^9\ M^{-1}$), the lines corresponding to equilibrium between octene isomers (a) and between phenyloctane isomers (b) were calculated by multiplying the experimentally obtained total selectivity to octenes or to phenyloctanes with the theoretical molar fractions of the individual octenes or phenyloctanes, in a mixture of octenes, respectively, in a mixture of phenyloctanes, at thermodynamic equilibrium. The equilibrium calculations were performed using thermodynamic data obtained from group contribution methods [43].

The selectivities to octene isomers as a function of 1-octene conversion (Fig. 4a) display the typical behavior of intermediately formed reaction products. 2-Octene is obtained with high selectivity at low 1-octene conversions (Fig. 4a) showing that the double bond isomerization occurs relatively fast as compared to the alkylation leading to phenyloctanes. The selectivity to 2-octene decreases steadily as the 1-octene conversion increases. However, the selectivities to 3-octene and 4-octene show an initial increase with 1-octene conversions. Due to subsequent transformations, a decrease of the selectivities of all octene

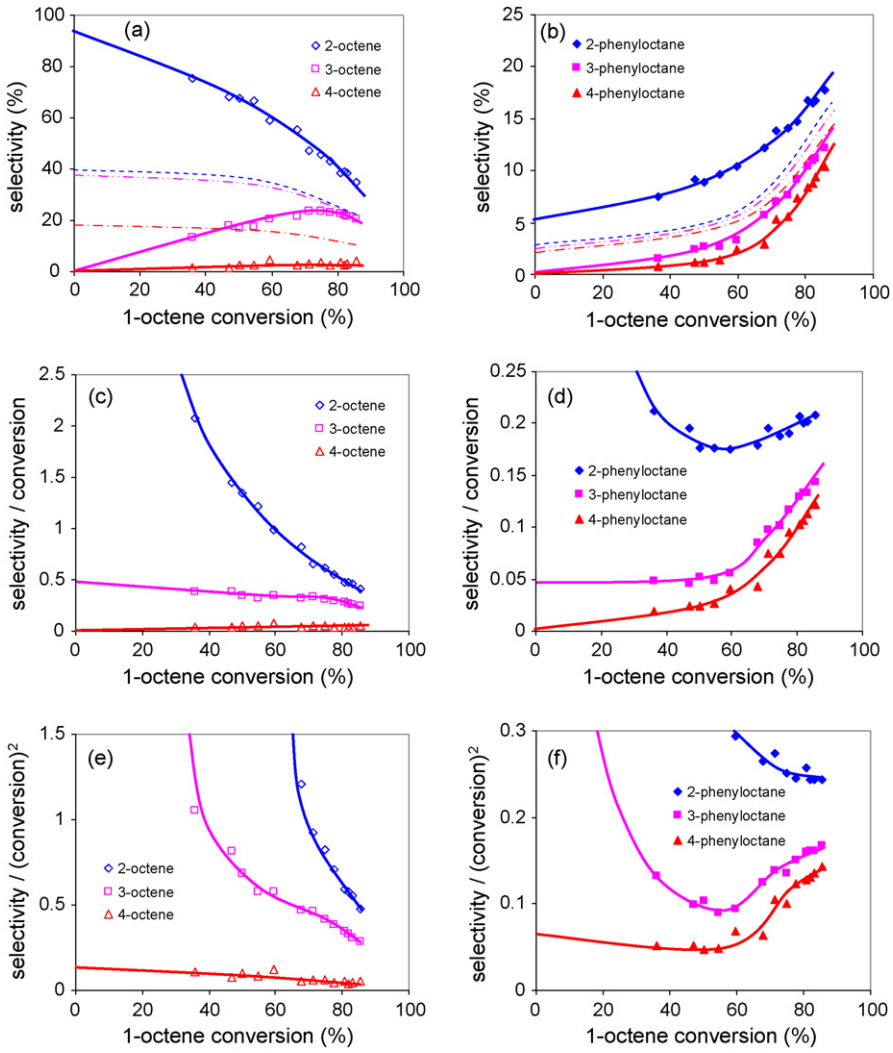

Fig. 4. First order (a and b), second order (c and d) and third order (e and f) delplot method charts for octene isomers (left) and phenyloctanes (right) for data over fresh CBV760 catalyst (t.o.s. = 0) at 343 K and benzene/1-octene molar feed ratio = 5. Symbols and solid lines correspond to experimental data, dotted lines (a and b) correspond to theoretical selectivities calculated for equilibrium between octene isomers (a), respectively, between phenyloctanes (b) (- - -), 2-isomer; (- · ·), 3-isomer; (- · -), 4-isomer.

isomers with increasing 1-octene conversion can be observed at high 1-octene conversion (Fig. 4a). Although the isomerization process is fast as compared to the alkylation, the internal equilibrium distribution of the octenes is not reached. Consequently, the double bond isomerization and the alkylation occur on comparable time scales and a proper interpretation of the observed product distributions requires that the two reactions – olefin isomerization and alkylation – are analyzed simultaneously.

For phenyloctanes, the selectivity increases as the 1-octene conversion increases at the expense of all olefins. The 2-phenyl-isomer is produced with the highest selectivity among the alkylated products. The steady increase in the selectivity to individual phenyloctane isomers (Fig. 4b) shows that these components do not suffer significant subsequent transformations at the experimental conditions investigated.

Based on the delplot technique, as presented by Bohre et al. [44], the primary, secondary or tertiary nature of the products can be determined based on plots of S_i, $S_i/X_{1\text{-oct}}$ and $(S_i/X_{1\text{-oct}})^2$ versus conversion. Primary reaction products are characterized by a non-zero first-rank delplot, i.e. the intercept of the plot of selectivity, S_i versus 1-octene conversion, while for all non-primary products a zero intercept is found. Secondary reaction products are characterized by a non-zero second-rank delplot, i.e. the intercept of the plot of selectivity $S_i/X_{1\text{-oct}}$ versus 1-octene conversion, while for primary products the intercept diverges and for tertiary products a zero intercept is found. Tertiary reaction products are characterized by a non-zero third-rank delplot, i.e. the intercept of the plot of selectivity $S_i/(X_{1\text{-oct}})^2$ versus 1-octene conversion, while for primary and secondary products the intercept diverges.

For each product, the plot of the selectivity S_i versus conversion is extrapolated to conversion zero ($X_{1\text{-oct}} \rightarrow 0$) as shown in Fig. 4a and b. Using 1-octene and benzene as feed, 2-octene and 2-phenyloctane are the only products with initial selectivities, i.e. obtained by extrapolation to zero conversion, different from zero. This observation suggests that 2-octene and 2-phenyloctane are the only primary products formed upon

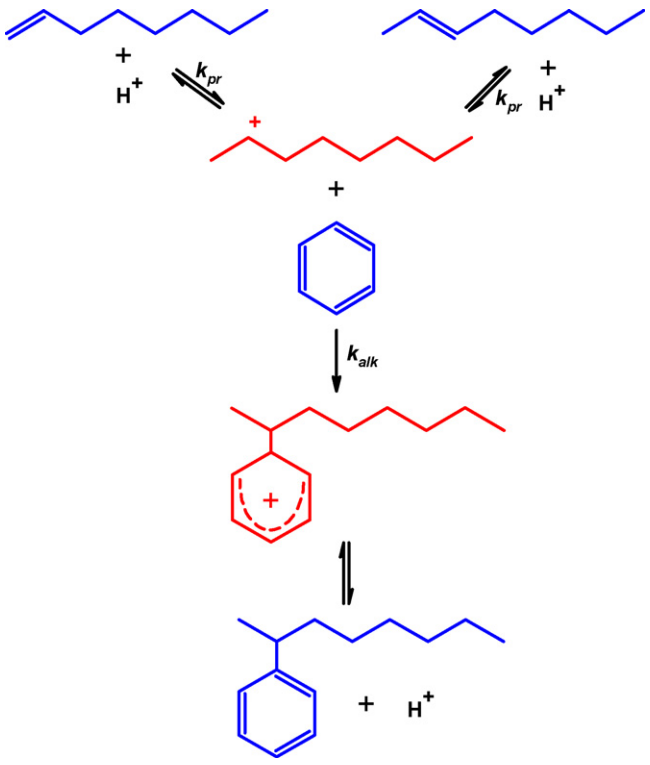

Scheme 3. Elementary reactions involved in the primary reaction network.

feeding benzene and 1-octene. Therefore, it can be concluded that the hydride shift elementary reactions do not occur significantly at the experimental conditions investigated since the internal rearrangements of the carbenium ion intermediates by 1,2-hydride shifts would allow the formation of all octene isomers and phenyloctanes directly, i.e. in parallel, from the 1-octene reactant. Consequently, the formation of octene isomers can be considered to occur mainly through a sequence consisting of consecutive protonation–deprotonation steps (see Scheme 2).

All the other components are formed as non-primary products since their initial selectivities are equal to 0. As evidenced by the high values of the equilibrium constants ($K \cong 10^9\ \mathrm{M}^{-1}$) for the formation of phenyloctanes from benzene and octenes, the alkylation reactions are practically irreversible at the experimental conditions investigated here and the primary reaction network can thus be described as presented in Scheme 3. Analogous to the findings of Smirniotis and Ruckenstein [45], Namuangruk et al. [46], and Corma et al. [14], for alkylation of benzene with short chain olefins, benzene adsorption is considered to be unimportant. Based on this primary network, the consumption rate of 1-octene is given by

$$R_{1\text{-oct}} = \frac{k_{pr}C_t\left[(C_{1\text{-oct}}K_{eq,iso} - C_{2\text{-oct}}) + (k_{alk}/k_{pr})K_{pr,1\text{-oct}}C_{1\text{-oct}}C_b\right]}{1 + K_{eq,iso} + K_{pr,1\text{-oct}}(C_{1\text{-oct}} + C_{2\text{-oct}}) + (k_{alk}/k_{pr})K_{pr,1\text{-oct}}C_b} \quad (11)$$

while the rate of formation of 2-octene and 2-phenyloctane can be expressed as

$$R_{2\text{-oct}} = \frac{k_{pr}C_t\left[(C_{1\text{-oct}}K_{eq,iso} - C_{2\text{-oct}}) - (k_{alk}/k_{pr})K_{pr,1\text{-oct}}C_{2\text{-oct}}C_b\right]}{1 + K_{eq,iso} + K_{pr,1\text{-oct}}(C_{1\text{-oct}} + C_{2-oct}) + (k_{alk}/k_{pr})K_{pr,1\text{-oct}}C_b} \quad (12)$$

$$R_{2\text{-pho}} = \frac{k_{alk}C_tK_{pr,1\text{-oct}}(C_{1\text{-oct}} + C_{2\text{-oct}})C_b}{1 + K_{eq,iso} + K_{pr,1\text{-oct}}(C_{1\text{-oct}} + C_{2\text{-oct}}) + (k_{alk}/k_{pr})K_{pr,1\text{-oct}}C_b} \quad (13)$$

Evaluating the ratio of the initial rates of formation of 2-octene and 2-phenyloctane, provides insight in the significance of the initial selectivity of 2-octene relative to the initial selectivity of 2-phenyloctane. For $X_{1\text{-oct}} \to 0$, Eqs. (12) and (13) can be simplified to

$$R^0_{2\text{-oct}} = \frac{k_{pr}C_tC_{1\text{-oct}}K_{eq,iso}}{1 + K_{eq,iso} + K_{pr,1\text{-oct}}C_{1\text{-oct}} + (k_{alk}/k_{pr})K_{pr,1\text{-oct}}C_b} \quad (14)$$

$$R^0_{2\text{-pho}} = \frac{k_{alk}C_tK_{pr,1\text{-oct}}C_{1\text{-oct}}C_b}{1 + K_{eq,iso} + K_{pr,1\text{-oct}}C_{1\text{-oct}} + (k_{alk}/k_{pr})K_{pr,1\text{-oct}}C_b} \quad (15)$$

The initial selectivity can then be expressed as

$$S^0_{2\text{-oct}} = \frac{R^0_{2\text{-oct}}}{R^0_{1\text{-oct}}} = \frac{k_{pr}K_{eq,iso}}{k_{pr}K_{eq,iso} + k_{alk}K_{pr,1\text{-oct}}C_b} \quad (16)$$

$$S^0_{2\text{-pho}} = \frac{R^0_{2\text{-pho}}}{R^0_{1\text{-oct}}} = \frac{k_{alk}K_{pr,1\text{-oct}}C_b}{k_{pr}K_{eq,iso} + k_{alk}K_{pr,1\text{-oct}}C_b} \quad (17)$$

leading to

$$\frac{S^0_{2\text{-oct}}}{S^0_{2\text{-pho}}} = \frac{k_{pr}K_{eq,iso}}{k_{alk}K_{pr,1\text{-oct}}C_b} = \frac{k_{pr}}{k_{alk}K_{pr,2\text{-oct}}C_b} = \frac{k_{de\text{-}pr}}{k_{alk}C_b} \quad (18)$$

From Eq. (18) it can be seen that the ratio of the initial selectivities is related to the ratio of the rate constant for the deprotonation step leading to the formation of 2-octene to the rate constant for alkylation leading to 2-phenyloctane. The observed higher initial selectivity of 2-octene as compared to the initial selectivity of 2-phenyloctane indicates that the rate constant for deprotonation is higher than the rate constant for alkylation.

The high yield of 2-phenyloctane, especially at low 1-octene conversion, is the consequence of this isomer being the only primary product among the alkylated products.

For each product, the plot of $S_i/X_{1\text{-oct}}$ and $S_i/(X_{1\text{-oct}})^2$ versus conversion is extrapolated to conversion zero ($X_{1\text{-oct}} \to 0$) as shown in Fig. 4c–e. Using 1-octene and benzene as feed, 3-octene and 3-phenyloctane are the only products with a non-zero intercept (see Fig. 4c and d); the intercept for 2-octene and 2-phenyloctane diverges while for 4-octene and 4-phenyloctane a zero intercept is found. Based on this observation, it can be concluded that only 2-octene transforms directly to 3-octene and

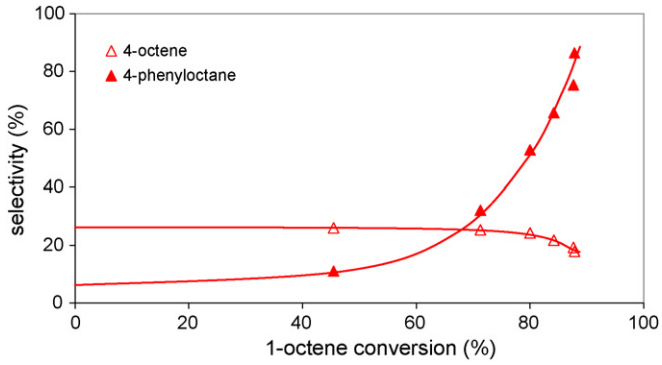

Fig. 5. Fresh catalyst (t.o.s. = 0) selectivity to 4-octene and 4-phenyloctane, calculated with respect to 1-octene, as a function of 1-octene conversion, when feeding benzene and mixture of octene isomers (benzene/octenes molar ratio = 5) over CBV760, at 358 K.

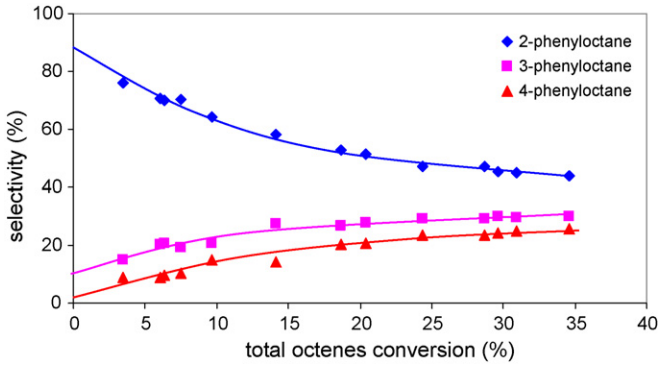

Fig. 6. Selectivity to phenyloctanes as a function of total olefin conversion over fresh CBV760 catalyst (t.o.s. = 0) at 343 K, benzene/1-octene molar feed ratio = 5.

3-phenyloctane. Therefore, 3-octene and 3-phenyloctane can be identified as being secondary products. Based Fig. 4e and f, it can be concluded that only 3-octene transforms directly to 4-octene and 4-phenyloctane. Therefore, 4-octene and 4-phenyloctane can be identified as being tertiary products when using 1-octene and benzene as feed.

At the investigated experimental conditions, 2-phenyloctane is formed directly from 1-octene while the formation of 3-phenyloctane and 4-phenyloctane depend on the intermediate formation of 2-octene and 3-octene, respectively. As the conversion of 1-octene increases, the internal distribution of the octene isomers evolves towards equilibrium driving the phenyloctanes towards a more homogeneous distribution (Fig. 4b). Corroborating evidence is obtained from a series of alkylation experiments using a mixture of octenes instead of pure 1-octene. The octenes feed consisted of a mixture of 22.4% 1-octene, 51.5% 2-octene, 25.9% 3-octene, 0.2% 4-octene. As shown in Fig. 5, 4-octene and 4-phenyloctane are also formed as primary products upon feeding an octene mixture that contains 3-octene.

In previous studies the double bond isomerization was not considered explicitly. Although the occurrence of double bond isomerization has been mentioned [16,20], no complete product distribution, including the olefin isomers, has been reported in the literature. In many cases, the internal distribution of the alkylated products is reported as a function of the total olefin consumption and not as a function of the conversion of the particular olefin isomer fed. Fig. 6, presents the selectivity to phenyloctanes as a function of total olefin conversion at 343 K for a molar ratio benzene/1-octene = 5. In contrast to Fig. 4, Fig. 6 does not yield any information on the olefin isomerization but also hampers the identification of the 2-phenyl-isomer as the unique primary product among the alkylated products in the case of feeding 1-olefins.

The above conclusions can be summarized in the reaction network shown in Scheme 4. In this reaction network, 1-octene transforms consecutively to the other octene isomers while all olefins can react in parallel with benzene and produce phenyloctanes. The observed low yields of 4-octene are justified as 4-octene is formed as a tertiary product when 1-octene is fed. The internal distribution of the phenyloctane isomers can be explained based on this reaction network without the need to invoke shape selectivity effects [42]. A high selectivity to 2-phenyloctane, as the only primary product among the phenyloctanes, can be expected if the isomerization path is relatively less important than the alkylation path.

4.3. Influence of temperature

In this study, three temperatures were investigated: 343 K, 358 K and 373 K. As illustrated in Fig. 2, the activity of the catalyst increases with increasing temperature. At 373 K, an almost complete 1-octene conversion ($X_{1\text{-oct}} > 99\%$) is reached even at relatively low space times while at 343 K, the reaction is slower and complete 1-octene conversion is not obtained at the investigated conditions.

As a function of space time (see Fig. 3), the molar yields of the three octene isomers pass through maximum values at

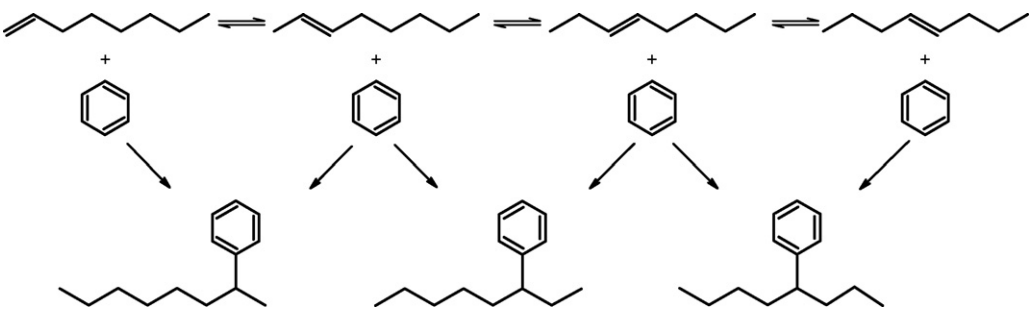

Scheme 4. Reaction network.

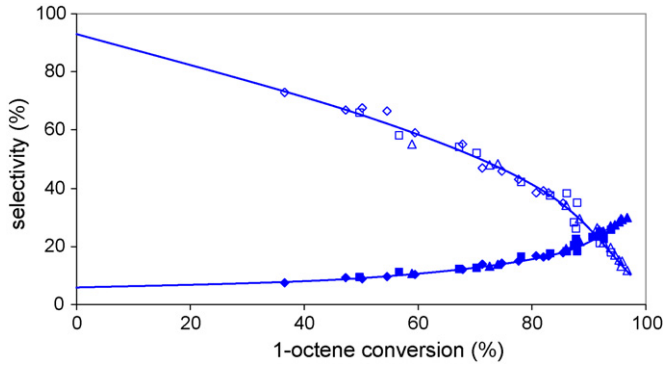

Fig. 7. Selectivity to 2-octene (empty symbols) and 2-phenyloctane (full symbols) as a function of 1-octene conversion over fresh CBV760 catalyst (t.o.s. = 0) at 343 K (diamonds), 358 K (squares) and 373 K (triangles), at benzene/1-octene feed molar ratio = 5.

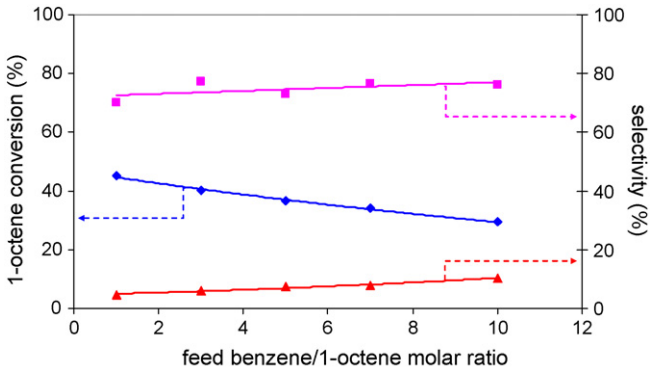

Fig. 8. Conversion of 1-octene (♦), selectivity to 2-octene (■) and selectivity to 2-phenyloctane (▲) as a function of the feed benzene to 1-octene molar ratio, over fresh CBV760 catalyst (t.o.s. = 0) at 343 K and $w_{cat}/F^0_{1\text{-oct}} = 10\,\text{kg s mol}^{-1}$.

all three temperatures investigated as expected for intermediary reaction products. With increasing temperature, the position of the maximum shifts towards lowers space times (see Fig. 3a and b). The molar yields of all alkylated products also increase with temperature.

As a function of 1-octene conversion, the overall selectivity to alkylated products (i.e. the sum of the selectivities of 2-, 3- and 4-phenyloctanes) and to octene isomers does not depend significantly on temperature. As illustrated in Fig. 7, the selectivity to the primary products, 2-octene and 2-phenyloctane, as a function of 1-octene conversion, is independent of temperature indicating that the deprotonation step leading to 2-octene has a similar activation energy as the alkylation step leading to 2-phenyloctane. From Eq. (18) it can be seen that the higher initial selectivity to 2-octene as compared to 2-phenyloctane can thus be related to differences in entropy of activation associated with deprotonation and with alkylation. At 358 K, a B/O molar ratio = 5 and a benzene concentration of 7835 mol m^{-3}, the observed initial selectivity ($X_{1\text{-oct.}} \rightarrow 0$) of 2-octene and 2-phenyloctane are 94% and 6%, respectively. Based on Eq. (18) a ratio of $A_{\text{de-pr}}/A_{\text{alk}} \approx 10^5$ can thus be estimated. Using statistical thermodynamics [47], the activation entropy was estimated according to the procedure described by Martens et al. [32]. An activation entropy of 43 J/mol K was calculated for the deprotonation step, while for the alkylation step the activation entropy amounted to −62 J/mol K leading to $A_{\text{de-pr}}/A_{\text{alk}} \approx 10^5/10^9 = 10^6$ in reasonable agreement with the experimentally determined ratio.

4.4. Influence of benzene to 1-octene feed ratio

In this study, benzene to 1-octene molar ratios of 1, 3, 5, 7 and 10 have been investigated and a summary of the results is presented in Fig. 8. The experiments were performed at low space time – 10 kg s mol^{-1} – to avoid the formation of polyalkylated aromatics at low benzene to 1-octene molar ratios. At the low space time investigated, 1-octene is mainly converted to other octene isomers.

High levels of 1-octene conversions were obtained at low benzene to 1-octene molar ratios. As the feed molar ratio increases from 1 to 10, the 1-octene conversion decreases from 45% to 29%. Simultaneously the yield of phenyloctanes increases slightly from 3% to 4%. The cumulative effect of this behavior is an almost doubling of the overall selectivity to alkylated products (from 7% to 13%) as the benzene to olefin feed ratio increases from 1 to 10. Higher benzene concentrations favor the alkylation path over the isomerization path. As a consequence of the primary product nature of 2-phenyloctane, when increasing the benzene to 1-octene molar ratio, the increase in the selectivity to this alkylated product is even more important than for the other phenyloctanes. Thus, 2-phenyloctane, that accounts for 70% of the phenyloctanes produced at 1:1 benzene to 1-octene feed molar ratio, accounts for 80% of the phenyloctanes obtained at 10:1 benzene to 1-octene feed molar ratio.

4.5. Influence of catalyst acid properties

To understand the effect of the catalyst acid properties and its performance in benzene alkylation, three USY zeolites with Si/Al ratio of 6, 13 and 30 were selected for this study. The dealumination process modifies the concentration of the acid sites of the zeolite by extracting Al atoms from its framework and alter its acid properties [35,48,49]. It is generally accepted that the average acid strength of the active sites of the zeolite increases with increasing zeolite Si/Al ratio up to a framework Si/Al ratio 6–8 as a result of the decreased number of Al atoms per unit cell achieved by dealumination [50]. Also, it has been shown that the simultaneous presence of Brønsted and Lewis acid sites can strongly influence the zeolite activity and selectivity in the alkylation of aromatics with alkenes [51]. The total concentration of acid sites of the catalysts amounted to 0.69, 0.64 and, respectively, 0.24 mmol acid site/g_{cat}, as determined from NH_3-TPD of CBV712, CBV720 and, respectively, CBV760 (see Table 1). Upon dealumination, the textural properties of the catalyst can also be modified by the creation of mesopores that, in some cases, improve the accessibility of the acid sites [18,50].

Even though the total number of acid sites for the three catalysts investigated decreases with increasing catalyst Si/Al_{bulk} ratio, catalyst activity, expressed in terms of 1-octene conversion, increases with increasing Si/Al_{bulk} ratio. Fig. 9 presents a direct comparison between the activities of the individual sites

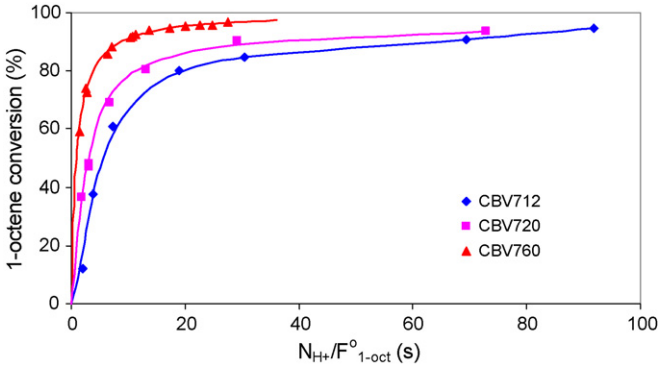

Fig. 9. Fresh catalyst (t.o.s. = 0) 1-octene conversion over three Y zeolite catalysts as a function of "site time" at 373 K and benzene/1-octene feed molar ratio = 5.

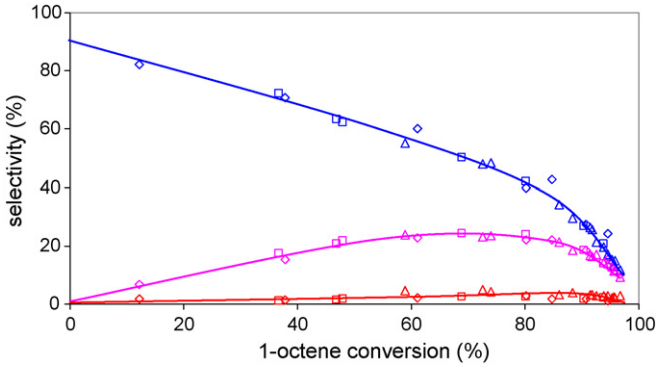

Fig. 11. Fresh catalyst (t.o.s. = 0) octene isomers distribution over the three Y zeolite catalysts as a function of 1-octene conversion, at 373 K and benzene/1-octene feed molar ratio = 5 (diamonds, CBV712; squares, CBV720; triangles, CBV760; blue, 2-octene, pink, 3-octene; red, 4-octene). (For interpretation of the references to colour in this figure legend, the reader is referred to the web version of the article.)

of each catalyst by plotting the conversion of 1-octene as a function of site time. CBV760 ($Si/Al_{bulk} = 30$) possesses the lowest number of acid sites in the series; however, the catalytic activity of these sites to transform 1-octene is higher than those of CBV720 ($Si/Al_{bulk} = 13$) and CBV712 ($Si/Al_{bulk} = 6$). The same kind of behavior has been observed previously in catalytic cracking and in hydrocracking over USY zeolites [16,18,34] and has been attributed to the positive influence of an increased average strength of the zeolite with increasing Si/Al_{bulk}.

Based on observations made for the liquid-phase alkylation of benzene with 1-dodecene over partially Na-exchanged HY-zeolites in a slurry–batch reactor, Dealmeida [16] suggested that an increase in acid strength leads to an increased alkylation activity and thus to an increased 2-phenyldodecane selectivity. Our results indicate that the selectivity to the reaction products depends only on the level of 1-octene conversion and is not influenced significantly by the zeolite acid properties. This observation pertains to the total selectivity to alkylated products and olefins, as presented in Fig. 10, as well as to the selectivity to each individual reaction product as illustrated in Figs. 11 and 12. Similar results on the influence of zeolite acid properties on the product selectivities have been reported in the case of hydrocracking [33] and catalytic cracking over zeolite catalysts [47,52]. However, as the olefin isomerization is not equilibrated, this study allows to trace back the influence of the zeolite acid properties to particular elementary steps in contrast to the case of hydrocracking and catalytic cracking where a straightforward evaluation of the influence of the Si/Al_{bulk} ratio on the activation energies of the elementary steps is complicated by equilibration of the protonation/deprotonation reactions [33,47].

The influence of the acid strength on the enthalpy diagram of the alkylation is illustrated in Fig. 13 for the formation of 2-phenyloctane. In principle, a change in acid strength can lead to a different concentration of carbenium ions on the catalyst surface due to a difference in stability of these ionic species that is reflected in a difference in the associated standard protonation enthalpies, ΔH_{pr}, and/or to a change in activation energy of the involved elementary reactions. For two catalysts A and B this can be represented as

$$\Delta(\Delta H_{pr}) = \Delta H_{pr,B} - \Delta H_{pr,A} \quad (19)$$

$$\Delta E_{a,pr} = E_{a,pr,B} - E_{a,pr,A} \quad (20)$$

$$\Delta E_{a,de\text{-}pr} = E_{a,de\text{-}pr,B} - E_{a,de\text{-}pr,A} \quad (21)$$

$$\Delta E_{a,alk} = E_{a,alk,B} - E_{a,alk,A} \quad (22)$$

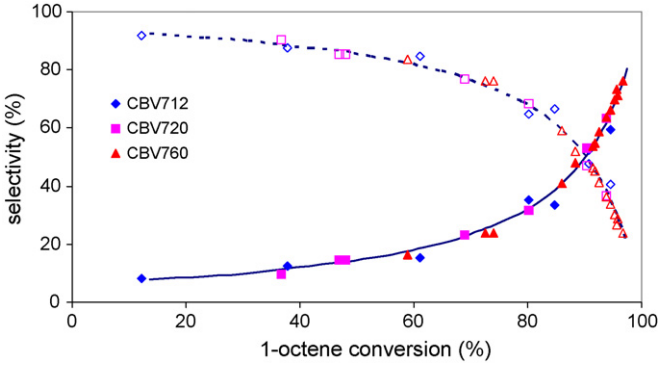

Fig. 10. Fresh catalyst (t.o.s. = 0) product distribution over three Y zeolite catalysts as a function of 1-octene conversion, at 373K and benzene/1-octene feed molar ratio = 5 (octenes, empty symbols and phenyloctanes, full symbols).

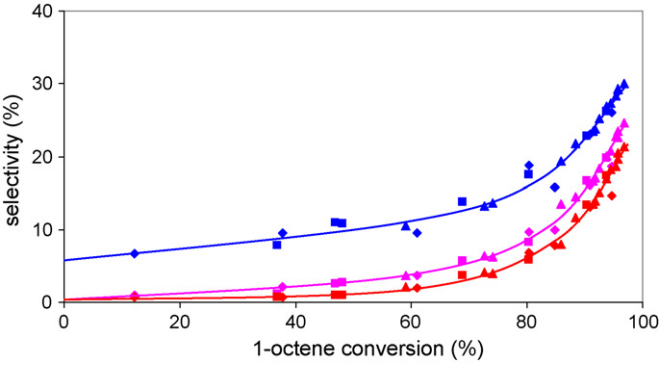

Fig. 12. Fresh catalyst (t.o.s. = 0) phenyloctane isomers distribution over the three Y zeolite catalysts as a function of 1-octene conversion, at 373K and benzene/1-octene feed molar ratio = 5 (diamonds, CBV712; squares, CBV720; triangles, CBV760; blue, 2-octene; pink, 3-octene; red, 4-octene). (For interpretation of the references to colour in this figure legend, the reader is referred to the web version of the article.)

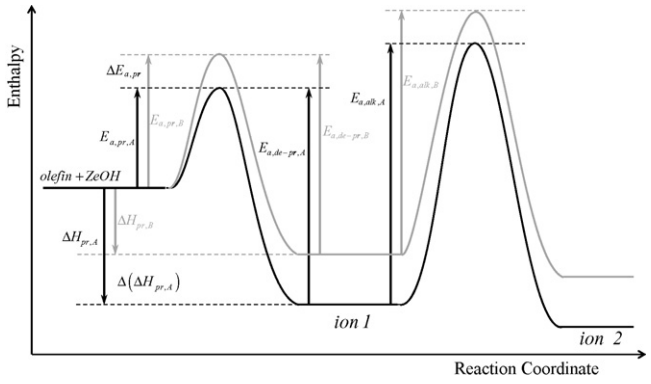

Fig. 13. Influence of the acid strength of the catalyst on the enthalpy diagram for the alkylation of benzene with 1-octene. Black line: stronger acid sites; grey line: weaker acid sites.

From Eq. (18), assuming that the pre-exponential factors are not influenced in going from one catalyst to another, the observed absence in selectivity differences can be expressed as

$$\frac{\exp(E_{\text{de-pr,A}})}{\exp(E_{\text{alk,A}})} = \frac{\exp(E_{\text{de-pr,B}})}{\exp(E_{\text{alk,B}})} \tag{23}$$

Leading to

$$\Delta E_{\text{a,de-pr}} = \Delta E_{\text{alk}} \tag{24}$$

Therefore, it can be concluded that the influence of a change in acid strength on the activation energy of the steps leading to the reaction products, i.e. deprotonation and alkylation, is independent from the type of elementary step.

As the activation energy for alkylation on two catalysts A and B can also be written as

$$E_{\text{a,alk,A}} = H_{\text{TSalk,A}} - H_{\text{ion1,A}} \tag{25}$$

$$E_{\text{a,alk,B}} = H_{\text{TSalk,B}} - H_{\text{ion1,B}} \tag{26}$$

the change in activation energy for alkylation in going from catalyst A to catalyst B is given by

$$\begin{aligned}\Delta E_{\text{a,alk}} &= (H_{\text{TSalk,B}} - H_{\text{TSalk,A}}) - (H_{\text{ion1,B}} - H_{\text{ion1,A}}) \\ &= \Delta H_{\text{TSalk}} - \Delta(\Delta H_{\text{pr}})\end{aligned} \tag{27}$$

From Eq. (27) it follows that the influence of the acid strength on the activation energy for alkylation depends not only on the stabilizing effect of the more acidic zeolite on the surface species but also on its stabilizing effect on the transition state. An increase in acid strength would result in an increase in activation energy for alkylation if the stabilizing effect on the intermediate were more pronounced than on the transition state.

In view of an Evans–Polanyi correlation, the change in the protonation and the deprotonation activation energy with acid strength is not independent from the change in the stability of the carbenium ions on the catalyst surface [52] with acid strength as reflected by $\Delta(\Delta H_{\text{pr}})$

$$\Delta E_{\text{a,pr}} = \alpha\Delta(\Delta H_{\text{pr}}) \tag{28}$$

$$\Delta E_{\text{a,de-pr}} = -(1-\alpha)\Delta(\Delta H_{\text{pr}}) = \Delta E_{\text{alk}} \tag{29}$$

Eq. (28) indicates that an increase in acid strength leads to an increased stability of the carbenium ions on the surface concomitant with a decrease in activation energy for protonation. From Eq. (29) it follows that for the catalyst with the higher average acid strength, the activation energies for the alkylation and deprotonation steps are higher then for the catalyst with the lower average acid strength.

Combining Eqs. (29) and (27) then leads to

$$\Delta H_{\text{TSalk}} = \alpha\Delta(\Delta H_{\text{pr}}) \tag{30}$$

From Eqs. (25) and (30) it can be concluded that an increased acid strength results in an increased stability not only of the intermediates formed on the zeolite surface but also of the transition state for alkylation. The increase in stability of the transition state is less pronounced and amounts to a fraction α of the increased stability of the surface species as reflected in $\Delta(\Delta H_{\text{pr}})$.

Our observations indicate that an increase in acid strength leads to an increased stabilization of the carbenium ions on the surface of the catalyst resulting in a decreased reactivity for desorption and alkylation of the surface species as the activation energy for these reaction steps increases. This decrease occurs to the same extent for the competing alkylation and deprotonation and, hence, to selectivity which is independent of acid strength.

Based on the above considerations, it can be concluded that the higher rates observed for the catalyst with the higher average acid strength are not related to an increase in the activity of the acid sites for the alkylation step but rather to a decrease in activation energy of the protonation steps (Eq. (28)) leading to an increased concentration of carbenium ions on the catalyst surface that compensates for the effect of the higher activation energies of the deprotonation and alkylation steps.

5. Conclusions

The liquid-phase alkylation of benzene with 1-octene at temperatures ranging from 343 K to 373 K over a series of Y zeolites, with Si/Al ranging from 6 to 30, was found to give two types of reaction products: octene isomers and phenyloctane isomers. Deactivation was found to be less important at 1-octene conversion >90% indicating that olefins are mainly responsible for the deactivation.

Based on carbenium ion chemistry a reaction network is presented. Reaction path analysis revealed that double bond isomerization and benzene alkylation occur on comparable time scales and thus require simultaneous consideration of all elementary steps involved. On the fresh catalyst, 2-octene and 2-phenyloctane were identified as being the only primary products formed indicating that olefin isomerization mainly occurs by a consecutive sequence of olefin protonation and deprotonation steps. Alkylation of the intermediately formed octyl carbenium ions occurs in parallel. The primary formation of 2-phenyloctane out of benzene and 1-octene explains the observed preferential formation of this phenyloctane isomer without the need to invoke shape selectivity effects.

It was observed that initial selectivities are independent of temperature. Based on the initial$_{(X\rightarrow 0\%)}$ rate equations, it can be

concluded that deprotonation and alkylation have similar activation energies and that a difference in entropy of activation associated with the deprotonation and the alkylation steps is responsible for the high selectivity to 2-octene as compared to 2-phenyloctane.

The highest activity per acid site was observed for the zeolite with the highest Si/Al ratio. The selectivities to the reaction products were not affected by a change in Si/Al ratio indicating that the influence of a change in acid strength is similar for the different types of elementary steps. The higher rates observed for the catalyst with the higher average acid strength can be explained by a change in activation energy of the elementary reaction steps. This change in activation energy can be related to the increased stability of the carbenium ions on the catalyst surface as reflected by $\Delta(\Delta H_{pr})$.

Acknowledgement

This research has been funded in the frame of the "HYPCAT" project (STWW 141) of the IWT of the Flemish Government.

References

[1] C. DeCastro, E. Sauvage, M.H. Valkenberg, W.F. Holderich, J. Catal. 196 (2000) 86.
[2] D. Dube, S. Royer, D.T. On, F. Beland, S. Kaliaguine, Microporous Mesoporous Mater. 79 (2005) 137.
[3] S. Sivasanker, A. Thangaraj, J. Catal. 138 (1992) 386.
[4] J.L. Berna Tejero, A. Moreno Danvila, US Patent 5,146,026 (1992) (to Petrochimica Espanola).
[5] J.A. Kocal, US Patent 5,196,574 (1993) (to UOP Inc.).
[6] C. Perego, S. Amarilli, A. Carati, C. Flego, G. Pazzuconi, C. Rizzo, G. Bellussi, Microporous Mesoporous Mater. 27 (1999) 345.
[7] A. de Angelis, S. Amarilli, D. Berti, L. Montanari, C. Perego, J. Mol. Catal. A: Chem. 146 (1999) 37.
[8] Z.G. Lei, C.Y. Li, B.H. Chen, W. Erqiang, J.C. Zhang, Chem. Eng. J. 93 (2003) 191.
[9] J.H. Clark, G.L. Monks, D.J. Nightingale, P.M. Price, J.F. White, J. Catal. 193 (2000) 348.
[10] S. Siffert, L. Gaillard, B.L. Su, J. Mol. Catal. A: Chem. 153 (2000) 267.
[11] G. Bellussi, G. Pazzuconi, C. Perego, G. Girotti, G. Terzoni, J. Catal. 157 (1995) 227.
[12] M.H. Han, Z. Cui, C. Xu, W. Chen, Y. Jin, Appl. Catal. A 238 (2003) 99.
[13] R.A. Innes, S.I. Zones, G.J. Nacamuli, US Patent 4,891,458 (1990) (to Chevron USA Inc.).
[14] A. Corma, V. Martinez-Soria, E. Schnoeveld, J. Catal. 192 (2000) 163.
[15] J.C. Cheng, T.F. Degnan, J.S. Beck, Y.Y. Huang, M. Kalyanaraman, J.A. Kowalski, C.A. Loehr, D.N. Mazzone, Sci. Technol. Catal. 121 (1999) 53.
[16] J.L.G. Dealmeida, M. Dufaux, Y.B. Taarit, C. Naccache, Appl. Catal. A 114 (1994) 141.
[17] B. Thomas, S. Sugunan, Microporous Mesoporous Mater. 72 (2004) 227.
[18] P. Meriaudeau, Y. BenTaarit, A. Thangaraj, J.L.G. Almeida, C. Naccache, Catal. Today 38 (1997) 243.
[19] Y. Cao, R. Kessas, C. Naccache, Y. Ben Taarit, Appl. Catal. A 184 (1999) 231.
[20] Z. Da, Z. Han, P. Magnoux, M. Guisnet, Appl. Catal. A 219 (2001) 45.
[21] P.T. Barger, G.J. Thompson, R.R. Herber, T. Imai, US Patent 4,774,377 (1988) (to UOP Inc.).
[22] J.M. Garces, J.J. Lee, M.M. Olken, J.J. Maj, A.Q. Campbell, G.M. Meima, M.J.M. Vanderaalst, M.S.U. Samson, Abstr. Pap. Am. Chem. Soc. 206 (1993) 69.
[23] J.F. Knifton, P.R. Anantaneni, P.E. Dai, M.E. Stockton, Catal. Today 79 (2003) 77.
[24] J.N. Armor, Appl. Catal. 78 (1991) 141.
[25] C. Perego, P. Ingallina, Catal. Today 73 (2002) 3.
[26] T.F. Degnan, C.M. Smith, C.R. Venkat, Appl. Catal. A 221 (2001) 283.
[27] J.L. Berna, L. Cavalli, C. Renta, Tenside Surfactants Detergents 32 (1995) 122.
[28] T. Imai, J.A. Kocal, B.V. Vora, Sci. Technol. Catal. 92 (1995) 339.
[29] Linear Alkylbenzenes (LAB), in: Nexant Report (2003).
[30] J.L. Berna, A. Moreno, J. Ferrer, J. Chem. Technol. Biotechnol. 50 (1991) 387.
[31] L. Cohen, R. Vergara, A. Moreno, J.L. Berna, J. Am. Oil Chem. Soc. 72 (1995) 115.
[32] G.G. Martens, G.B. Marin, J.A. Martens, P.A. Jacobs, G.V. Baron, J. Catal. 195 (2000) 253.
[33] J.W. Thybaut, G.B. Marin, G.V. Baron, P.A. Jacobs, J.A. Martens, J. Catal. 202 (2001) 324.
[34] E. Collignon, M. Mariani, S. Moreno, M. Remy, G. Poncelet, J. Catal. 166 (1997) 53.
[35] F. Collignon, G. Poncelet, J. Catal. 202 (2001) 68.
[36] J.F.M. Denayer, J.A. Martens, P.A. Jacobs, J.W. Thybaut, G.B. Marin, G.V. Baron, Appl. Catal. A 246 (2003) 17.
[37] M.J. Remy, D. Stanica, G. Poncelet, E.J.P. Feijen, P.J. Grobet, J.A. Martens, P.A. Jacobs, J. Phys. Chem. 100 (1996) 12440.
[38] http://www.autoclaveengineers.com.
[39] R.J. Berger, E.H. Stitt, G.B. Marin, F. Kapteijn, J.A. Moulijn, Cattech 5 (2001) 30.
[40] M. Guisnet, P. Magnoux, Appl. Catal. 54 (1989) 1.
[41] M. Guisnet, P. Magnoux, Catalyst Deactivation 88 (1994) 53.
[42] W.G. Liang, Y. Jin, Z.Q. Yu, Z.W. Wang, B.B. Han, M.Y. He, E.Z. Min, Zeolites 17 (1996) 297.
[43] R.C. Reid, J.M. Prausnitz, B.E. Poling, The Properties of Gases and Liquids, McGraw-Hill Book Company, New York, 1987, P.
[44] N.A. Bhore, M.T. Klein, K.B. Bischoff, Ind. Eng. Chem. Res. 29 (1990) 313.
[45] P.G. Smirniotis, E. Ruckenstein, Ind. Eng. Chem. Res. 34 (1995) 1517.
[46] S. Namuangruk, P. Pantu, J. Limtrakul, J. Catal. 225 (2004) 523.
[47] G. Yaluris, J.E. Rekoske, L.M. Aparicio, R.J. Madon, J.A. Dumesic, J. Catal. 153 (1995) 54.
[48] W.M. Zhang, E.C. Burckle, P.G. Smirniotis, Microporous Mesoporous Mater. 33 (1999) 173.
[49] H. Miessner, H. Kosslick, U. Lohse, B. Parlitz, V.A. Tuan, J. Phys. Chem. 97 (1993) 9741.
[50] D. Barthomeuf, Mater. Chem. Phys. 17 (1987) 49.
[51] J. Čejka, B. Wichterlova, Catal. Rev. 44 (2002) 375;
B.A. Watson, M.T. Klein, R.H. Harding, Ind. Eng. Chem. Res. 35 (1996) 1506.
[52] J.A. Dumesic, D.F. Rudd, L.M. Aparicio, J.E. Rekoski, A.A. Trevino, The Microkinetics of Heterogeneous Catalysis, American Chemical Society, Washington, DC, 1993, p. 41.